This is the author's version of an article that has been published. Changes were made to this version by the publisher prior to publication. The final version of record is available at https://dx.doi.org/10.1109/EEE-AM58328.2023.10395325

Robust Disturbance Rejection Control of DC/DC Interleaved Boost Converters with Additional Sliding Mode Component

Antonino Sferlazza
Department of Engineering
University of Palermo
Palermo, Italy
antonino.sferlazza@unipa.it

Giovanni Garraffa
Faculty of Engineering and Architecture
University of Enna Kore
Enna, Italy
giovanni.garraffa@unikore.it

Gianpaolo Vitale
Istituto di Calcolo e reti ad Alte pRestazioni (ICAR)
National Research Council of Italy (CNR)
Palermo, Italy
gianpaolo.vitale@icar.cnr.it

Filippo D'Ippolito
Department of Engineering
University of Palermo
Palermo, Italy
filippo.dippolito@unipa.it

Francesco Alonge
Department of Engineering
University of Palermo
Palermo, Italy
francesco.alonge@unipa.it

Giuseppe Lullo
Department of Engineering
University of Palermo
Palermo, Italy
giuseppe.lullo@unipa.it

Alessandro Busacca
Department of Engineering
University of Palermo
Palermo, Italy
alessandro.busacca@unipa.it

Giuseppe Costantino Giaconia
Department of Engineering
University of Palermo
Palermo, Italy
costantino.giaconia@unipa.it

Daniele Scirè
Department of Engineering
University of Palermo
Palermo, Italy
daniele.scire@unipa.it

***Abstract*—Interleaved DC/DC boost converters are nowadays widely studied due to their properties of reducing the current ripple and increasing fault tolerance. This paper describes a control method that allows good output voltage regulation, together with robustness against parameter uncertainties, deviation of the supply voltage of the source, and load deviation. These objectives are obtained by determining an equivalent circuital scheme of the interleaved boost and associating to this scheme a linear mathematical model by means of the exact linearization method. Subsequently, trajectory tracking control techniques are employed based on disturbance compensation and a sliding mode component is added to cope with parameter uncertainties and possible compensation errors. The controller, applied to the above equivalent conventional boost model, allows to command the duty cycle of single phases of the Mosfets. This controller uses the output voltage and the currents flowing in the phases of the converter as feedback variables. Simulation results show the validity of the proposed approach.**

***Index Terms*—Interleaved converter, trajectory tracking, active disturbance rejection control, feedback linearization, robustness through sliding mode component.**

I. Introduction

Interleaved DC/DC boost converters are widely studied nowadays, as they appear in the specialized literature, due to their peculiarities of reducing the current ripple at the input and output and their fault tolerance property. As is well known, the interleaving conversion is realized by connecting some cells having the same structure, operating at the same switching frequency, but the successive switching instants are delayed for the same amount of time equal to the switching period divided by the number of cells. Moreover, the above structure shares the same source, the output capacitor, and the load [1]. Alternative solutions to the interleaved converters are represented by quadratic boost converters with non-conventional topologies or boost conveters controlled by suitable control techniques where all variables (both voltages and currents) are contemporary controlled in order to avoid overshoots or very high ripples [2]–[4].

Regarding the control method used for interleaved converters, besides those based on the classical PI control, it is convenient to consider more efficient control methods based on state-space modeling. In [1], a two-phase interleaved boost is studied for application in discontinuous conduction mode (DCM) to obtain high efficiency and reduce the diode losses. The control strategy consists of two control loops: the PI regulator controls the outer output voltage loop and gives the desired currents, whereas the inner control loop is controlled through the bang-bang method. In [5], N identical boosts are connected in parallel to force the output voltage to the desired value, reducing the ripple in the input current and output voltage. The control of the converter is performed by comparing the currents flowing in the phases of the converter itself and evaluating if the difference between their values is greater or smaller than a chosen value. The results of this comparison determine which phase must be activated to compensate for the ripple. It follows that the controller is static and does not consider the converter's dynamics. State-space modeling of an interleaved boost converter is illustrated in [6]. In particular, the matrices of the dynamical model depend on the duration of the different conduction configurations that can

This research was funded by:
- The SiciliAn MicronanOTecH Research and Innovation CEnter "SAMOTHRACE" (MUR, PNRR-M4C2, ECS_00000022), spoke 3-Università degli Studi di Palermo "S2-COMMs-Micro and Nanotechnologies for Smart & Sustainable Communities,
- The European Project GaN4AP (Gallium Nitride for Advanced Power Applications). The project has received funding from the Electronic Component Systems for European Leadership Joint Undertaking (ECSEL JU), under grant agreement No.101007310. This Joint Undertaking receives support from the European Union's Horizon 2020 research and innovation programme, and Italy, Germany, France, Poland, Czech Republic, Netherlands.

appear in the converter according to the different status of the switches and diodes. This model is used to study the converter at the steady state and does not help the design of control algorithms. In [7], an interleaved two-phase DC/DC boost converter is studied in a wider contest regarding the plug-in hybrid electric vehicle applications. The control is performed in the frequency domain, using a simplified transfer function from duty-cycle to voltage and duty-cycle to current. In [8], a high-efficiency two-phase boost converter is described for DC microgrid applications. The converter is modeled in the state space contest, whereas the controller design is performed in the frequency domain. In [9], it is shown that an N-phases interleaved boost with all the inductances of the same value can be studied considering a conventional equivalent boost where the inductances and the associated parasitic resistances are N times lower than those of the interleaved circuit. In [10], the conventional equivalent boost is employed for designing a controller, which is then extended to the interleaved boost control. The equivalent boost is controlled by applying the backstepping procedure to a model obtained via the exact feedback linearization method illustrated in [11]. In [12], a nonlinear controller is designed via a backstepping approach so that the current of the N-phases of the interleaved converter follows the reference current, which is assumed with the same value. In this way, if the load resistance and the input voltage are perfectly known, the output voltage also assumes the desired value. However, the load resistance is estimated via a parameter adaptation mechanism, whereas the input voltage cannot be accessible for the measurement. Consequently, controlling the current to the desired value could not produce the desired output voltage. Finally, some literature works focused on the analysis and modeling of DC-DC boost converters in interleaving configurations exploiting inductors in the quasi-saturation region in order to optimize the power density by minimizing the size of the inductors [13], [14].

This paper deals with the control of a N-phases interleaved boost converter with all the phases having the same inductors and, consequently, the same value of inductance and parasitic resistance. Moreover, all the phases share input supply voltage, output capacitor, and load resistance. The controller design aims to guarantee the output voltage regulation, with all the phase currents of the same value, and to obtain the maximum ripple reduction both at the input and the output, as proposed in [12]. The controller design starts from the conventional boost equivalent model to the interleaved multi-phase boost, illustrated in [9], followed in [10]. However, instead of using the second-order model corresponding to the equivalent boost model, as in [10] and [12], a model with dynamic input is derived assuming the duty-cycle as a further state variable computed by integration of an auxiliary control variable. The resulting model is of third order and can be linearized using a suitable transformation. Based on this linearized model, a nonlinear controller is constructed to force the closed loop system to track a trajectory in the state space of the linearized model, consisting of the reference output and its first three derivatives. Finally, according to the method illustrated in [15] (see pp.285 and following), a sliding mode component is added to the control previously described to take explicitly into account all the uncertainties, thus gaining the robustness of the closed loop system. A similar approach was recently used to control a quadratic boost converter [16]. However, to the best of the author's knowledge, this approach has never been applied to the interleaved boost converter in other literature works.

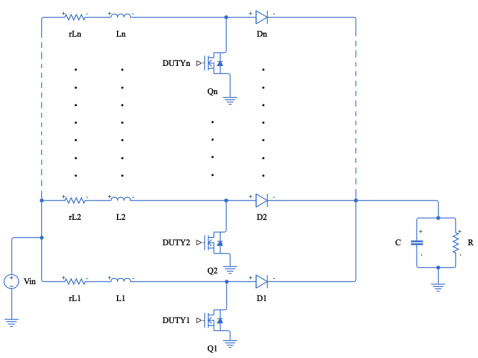

Fig. 1. Electrical circuit of the N-Phases interleaved boost converter.

II. Dynamic Model of the N-Phases Interleaved Boost Converter

The electrical circuit of the N-Phases interleaved boost converter is shown in Fig. 1. Assuming that the boost converter is designed for continuous conduction mode and neglecting the parasitic resistance of the capacitor, it can be described through the state space mathematical model given by:

$$\dot{i}_{L_i} = \frac{1}{L_i}\left(-r_{L_i} i_{L_i} - (1-u_i)v_C + V_{in}\right), \quad i=1,\cdots,N \quad (1)$$

$$\dot{v}_C = \frac{1}{C}\sum_{i=1}^{N}(1-u_i)i_{L_i} - \frac{1}{RC}v_C, \qquad i=1,\cdots,N \quad (2)$$

where $u_i \in \{0,1\}$ ($u_i = 0$ if the switch is in the OFF state and $u_i = 1$ if the switch is in the ON state). This model describes the controller in all the working conditions. However, for designing a controller, it is convenient to associate with this model an averaged model obtained substituting to the discontinuous inputs u_i a continuous input $\lambda_i \in [0,1]$. Note that some symmetry conditions are considered in this model. For example, all the phases have the same inductors, i.e. the inductances and the parasitic resistances have the same values, L and r_L respectively and, in a generic sampling period T_s, the same value of λ is applied to all the N-phases, although the command signals applied to the gates of the MOSFETs are delayed by $\frac{T_s}{N}$ each other. The corresponding averaged dynamical model is given by:

$$\dot{i}_{L_i} = \frac{1}{L_i}(-r_{L_i} i_{L_i} - (1-\lambda)v_C + V_{in}), \quad (3)$$

$$\dot{v}_C = \frac{1}{C}\left(\sum_{i=1}^{N}(1-\lambda)i_{L_i} - \frac{1}{R}v_C\right). \quad (4)$$

The equilibrium state corresponding to a generic value λ_e, is obtained putting $\dot{i}_{L_i} = \dot{v}_C = 0$, $i = 1, \cdots, N$, $r_{L_i} = r_L$ and $L_i = L$ and summing the resulting equations (3), as follows:

$$-r_L \sum_{i=1}^{N} i_{L_i,e} - (1-\lambda_e) N v_{C,e} + N V_{in} = 0, \tag{5}$$

$$(1-\lambda_e) \sum_{i=1}^{N} i_{L_i,e} - \frac{1}{R} v_{C,e} = 0. \tag{6}$$

From (5) and (6), the equilibrium state becomes:

$$\sum_{i=1}^{N} i_{L_i,e} = \frac{N V_{in}}{r_L + NR(1-\lambda_e)^2}, \tag{7}$$

$$v_{C,e} = \frac{NRV_{in}(1-\lambda_e)}{r_L + NR(1-\lambda_e)^2}. \tag{8}$$

Equation (7) shows that the equilibrium state regarding the current is not unique. However, if the symmetry conditions explained before are considered, the equilibrium state is well-defined for each phase, and it is given by:

$$i_L = \frac{V_{in}}{r_L + NR(1-\lambda_e)^2}. \tag{9}$$

III. Control of the N-phases interleaved boost converter

The control of the interleaved boost converter using model (3)-(4) is not trivial because of the interaction among the phases. However, considering the assumptions made at the end of the previous Section, a procedure based on the equivalent mono-phase boost converter model can be used for designing the controller. This model is described by the following equations:

$$\dot{i}_L = \frac{1}{L_{eq}}(-r_{L_{eq}} i_L - (1-\lambda) v_C + V_{in}), \tag{10}$$

$$\dot{v}_C = \frac{1}{C}\left((1-\lambda) i_L - \frac{1}{R} v_C\right). \tag{11}$$

The control procedure can be schematized as follows:

- *A.* The mono-phase equivalent boost model is linearized using a suitable nonlinear transformation of variables;
- *B.* A control law is designed in order to force the linearized model to track a desired trajectory in its state space, and an extended state observer is considered to estimate the external disturbance, which has to be compensated for linearizing the model.
- *C.* A sliding mode component is designed to cope with parameter uncertainties and possible compensation errors, and the duty cycle obtained is, finally, applied to the interleaved converter with a suitable delay among phases.

A. Exact linearization of the mono-phase equivalent boost model

In this paper, the linearization is performed on the dynamical model of the converter with dynamic input of integral type, putting $r_L = 0$. This type of model is essential because the integrator has a stabilization effect (see [17] and reference therein). The model of the mono-phase equivalent boost with dynamic integral input is obtained by extending the state of model (10)-(11) by adding the equation:

$$\dot{\lambda} = \delta, \tag{12}$$

where δ is the auxiliary input. In this way, the converter control variable λ is assumed to be a third state variable. The control variable λ is then computed by integrating the auxiliary control input δ, and consequently, its high-frequency components can be conveniently filtered. Defining:

$$z_1 = C v_C^2 + L i_L^2, \tag{13}$$

as the output of the linearized model, the Brunovski canonical form can be written as follows:

$$\dot{\boldsymbol{z}} = \boldsymbol{A}_z \boldsymbol{z} + \boldsymbol{b}_z \mu \tag{14}$$

$$y_z = z_1 \tag{15}$$

where:

$$\boldsymbol{A}_z = \begin{bmatrix} 0 & 1 & 0 \\ 0 & 0 & 1 \\ 0 & 0 & 0 \end{bmatrix}, \boldsymbol{b}_z = \begin{bmatrix} 0 \\ 0 \\ 1 \end{bmatrix},$$

$$\mu = \alpha\delta + \eta, \tag{16}$$

$$\alpha = 2\left(\frac{V_{in}}{L} + \frac{2}{RC} i_L\right) v_c, \tag{17}$$

$$\eta = \frac{8}{R^2 C} v_C \dot{v}_C - 2(1-\lambda)\left(\frac{V_{in}}{L}\dot{v}_C + \frac{2}{RC}(\dot{v}_C i_L + v_C \dot{i}_L)\right). \tag{18}$$

where η is considered as an endogenous disturbance.

B. Control law for the linearized model

The Brunovski canonical form previously illustrated is controllable and leads to the following input-output model:

$$\dddot{y}_z = \mu. \tag{19}$$

The control law for model (19) is obtained from the following result.

Proposition 1: The control law given by:

$$\mu = \dddot{z}_{1,ref} - \gamma_{z2}(\ddot{z}_1 - \ddot{z}_{1ref}) - \gamma_{z1}(\dot{z}_1 - \dot{z}_{1ref}) - \gamma_{z0}(z_1 - z_{1ref}). \tag{20}$$

induces asymptotic stability to dynamics (19) if the polynomial $s^3 + \gamma_{z2} s^2 + \gamma_{z1} s + \gamma_{z0} = 0$ is Hurwitz.

Proof. Putting $e_{yz} = y_z - y_{z,ref}$, substituting (20) into (19), the following equation is obtained:

$$\dddot{e}_{yz} + \gamma_{z2}\ddot{e}_{yz} + \gamma_{z1}\dot{e}_{yz} + \gamma_{z0} e_{yz} = 0, \tag{21}$$

which implies that $\lim_{t\to\infty} e_{yz} = 0$ if the hypotesis is satisfied.

Note that for processing the control law (20), it is necessary to know the first and second derivatives of y_z since the derivatives of $y_{z,ref}$ are all equal to zero. Moreover, since the objective is determining the plant input δ by inverting (16),

$$\delta = \alpha^{-1}(\mu - \eta), \tag{22}$$

estimating the disturbance η is also necessary. The above objectives can be reached using a linear extended state observer (LESO).

The LESO for the model (14) is given by:

$$\dot{\hat{z}}_1 = \hat{z}_2 + \epsilon^{-1}\beta_1 e_z, \tag{23}$$

$$\dot{\hat{z}}_2 = \hat{z}_3 + \epsilon^{-2}\beta_2 e_z, \tag{24}$$

$$\dot{\hat{z}}_3 = \hat{z}_4 + \epsilon^{-3}\beta_3 e_z + \alpha\delta, \tag{25}$$

$$\dot{\hat{z}}_4 = \epsilon^{-4}\beta_4 e_z, \tag{26}$$

where $e_z = z_1 - \hat{z}_1$, the parameters β_i, $i = 1, \ldots, 4$ are usually selected as the coefficients (in decreasing order) of the polynomial $(s+\omega_0)^4$ where ω_0 is a suitable chosen parameter (cf. for example [18]). Moreover, in [19], it is shown that if $|\eta|$ and $|\dot{\eta}|$ are bounded, the state of the following dynamic model converges to a ball whose radius depends on ϵ and increases at the increasing of ϵ. Note the $\hat{z}_4$ corresponds with the estimated value of η.

C. Design of the sliding mode component

Another problem is due to the computation of the control gain α in (17), which depends on the circuital parameters, including the supply voltage V_{in}, the state variables v_C and i_L, and, consequently, errors due to uncertainty could be introduced in the control law. To cope with these problems, it is convenient to introduce a sliding control component in the control law, which gives robustness to the whole system. This component is provided by:

$$u_{sm} = -k\text{sign}(s), \tag{27}$$

where $\text{sign}(s)$ is the signum function and:

$$s = \ddot{e}_{yz} + k_1\dot{e}_{yz} + k_0 e_{yz}, \tag{28}$$

is the sliding function.

The gain k is obtained taking into account explicitly the parameter deviations. In particular, assuming to know the minimum and maximum values for α, α_m and α_M, respectively, the quantities $\hat{\alpha} = \sqrt{\alpha_m \alpha_M}$ and $\beta = \sqrt{\frac{\alpha_M}{\alpha_m}}$ can be determined, and it is easy to verify that both $\frac{\hat{\alpha}}{\alpha}$ and $\frac{\alpha}{\hat{\alpha}}$ belong to the interval $[\beta^{-1}, \beta]$.

Then, by choosing $V(s) = 0.5s^2$, its derivative is negative definite if the following inequality is satisfied:

$$s\dot{s} \leq -\rho s,$$

for any positive constant ρ, or, equivalently, if:

$$\dot{s}\text{sign}(s) \leq -\rho. \tag{29}$$

Inequality (29) is satisfied if k is chosen such that

$$k \geq |\mu - \hat{z}_4| + \epsilon_\eta\beta|\hat{z}_4| + \beta|\hat{z}_4 + k_1\ddot{z}_1 + k_0\dot{z}_1 + \rho|, \tag{30}$$

where it is assumed that $\frac{|\eta - \hat{\eta}|}{|\hat{\eta}|} \leq \epsilon_\eta$, and taking into account that the derivatives of $y_{z,ref}$ are equal to zero. The reader is addressed to [15] for further details.

Finally, the control law is given by:

$$\delta = \frac{1}{\hat{\alpha}}(\mu - \hat{z}_4 + u_{sm}), \tag{31}$$

where $\hat{z}_4$ is the estimated value of η by means of the LESO and u_{sm} is given by (27).

The duty cycle λ, as already said, is obtained by integrating δ. Finally, once the value of λ is determined, it is applied to all n-phases of the boost interleaved. Naturally, the periods among the phases are suitably delayed by $\frac{Ts}{N}$ seconds, where T_s is the modulation period, and N is the number of phases.

IV. Simulation experiments

To test the behavior of the interleaved boost converter, simulation experiments are performed considering $N = 4$, and the following values of the parameters: $V_{in} = 24$ V, $L = 470\mu H$, $C = 30\mu F$, $R = 37.5\Omega$, $r_L = 10m\Omega$ and $r_C = 10m\Omega$. The employed components have the following tolerances: $\pm 20\%$ for inductances, $\pm 10\%$ for the capacity. Moreover, it is assumed that V_{in} and R can vary of $\pm 20\%$ and $\pm 30\%$, respectively. The boost converter, the LESO, and the controller are implemented in the Matlab/Simulink environment (Simscape is used to simulate the interleaved boost converter).

A first experiment considers a start-up transient with $V_{C,ref} = 100$ V, and it considers nominal parameters, i.e. the parameters used to design the controller are precisely the same as the simulated model. The simulation results are given in Fig.2.

The results show that for nominal parameters, the output voltage, Fig. 2(a), converges towards the reference one after a transient of about 35 ms. Moreover, as shown in 2(c), the estimation of the endogenous disturbance converges towards the computed one in about 10 ms. This confirms that both controller and LESO are working correctly and the total disturbance is adequately compensated. Regarding the other variables, it is possible to note that the duty cycle, 2(b), has a coherent waveform with the behavior of the output voltage. Finally, Fig. 2(d) shows input current, and Fig.s 2(e) and 2(f) show the currents on the four phases. In particular, Fig. 2(f) shows their steady-state values in the 40 μs interval. As the interleaved converter requires, the four-phase currents are delayed by 5 μs each other.

Compared to the conventional equivalent boost converter, the ripple in the input current, shown in Fig. 2(d) is 0.8 A peak-to-peak instead of 1.3 A, and the output voltage ripple is 1 V peak-to-peak instead of 2 V, besides, it exhibits a higher frequency, this proves the effectiveness of the interleaved configuration.

To evaluate the robustness of the closed-loop control system, a second test is carried out considering, at the same time, a variation of the input voltage of -20%, a mismatch of the inductances: $L_1 = 1.2L$, $L_2 = 0.8L$, $L3 = 0.8L$ and $L_4 =$

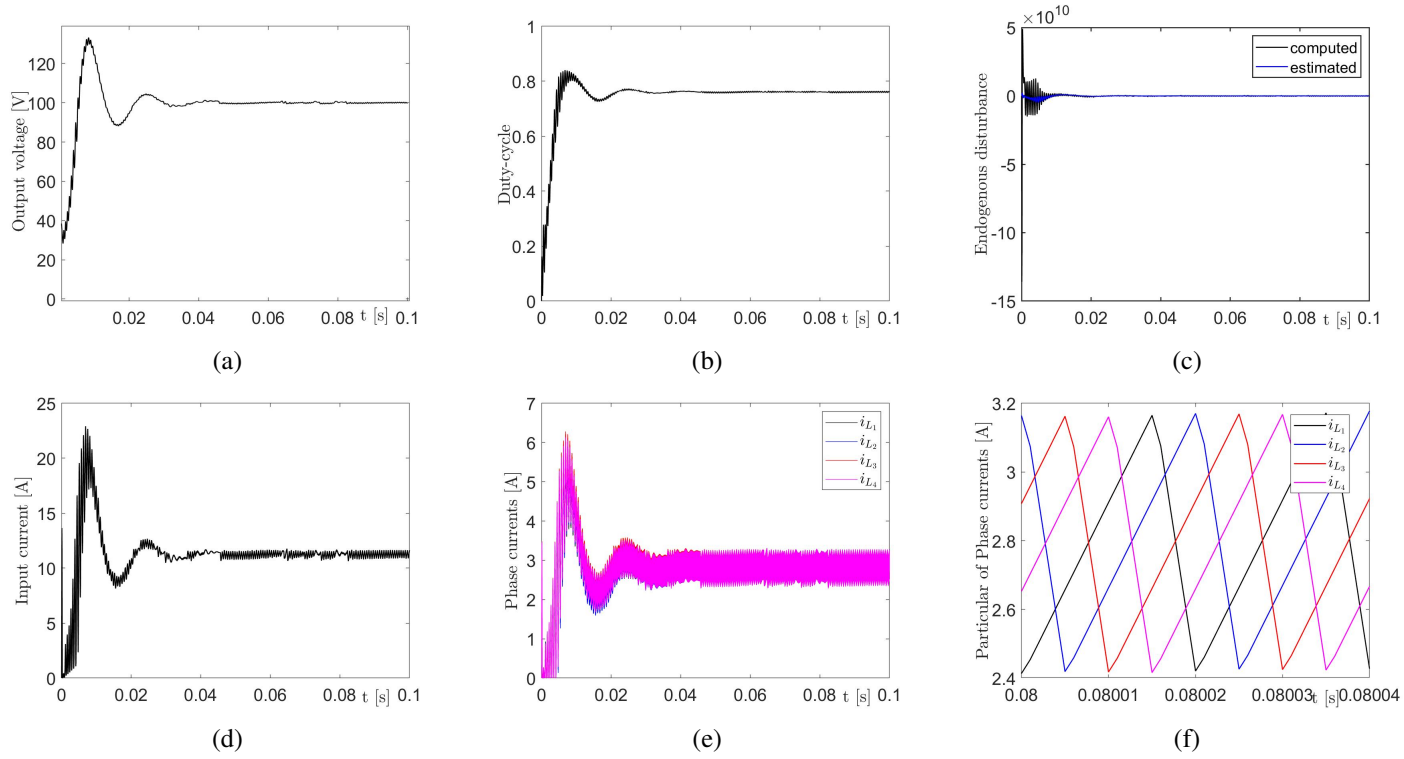

Fig. 2. Test under nominal parameters: (a) output voltage; (b) duty cycle; (c) computed and estimated disturbance; (d) input current; (e) phase currents; (f) steady-state waveforms of the phase currents.

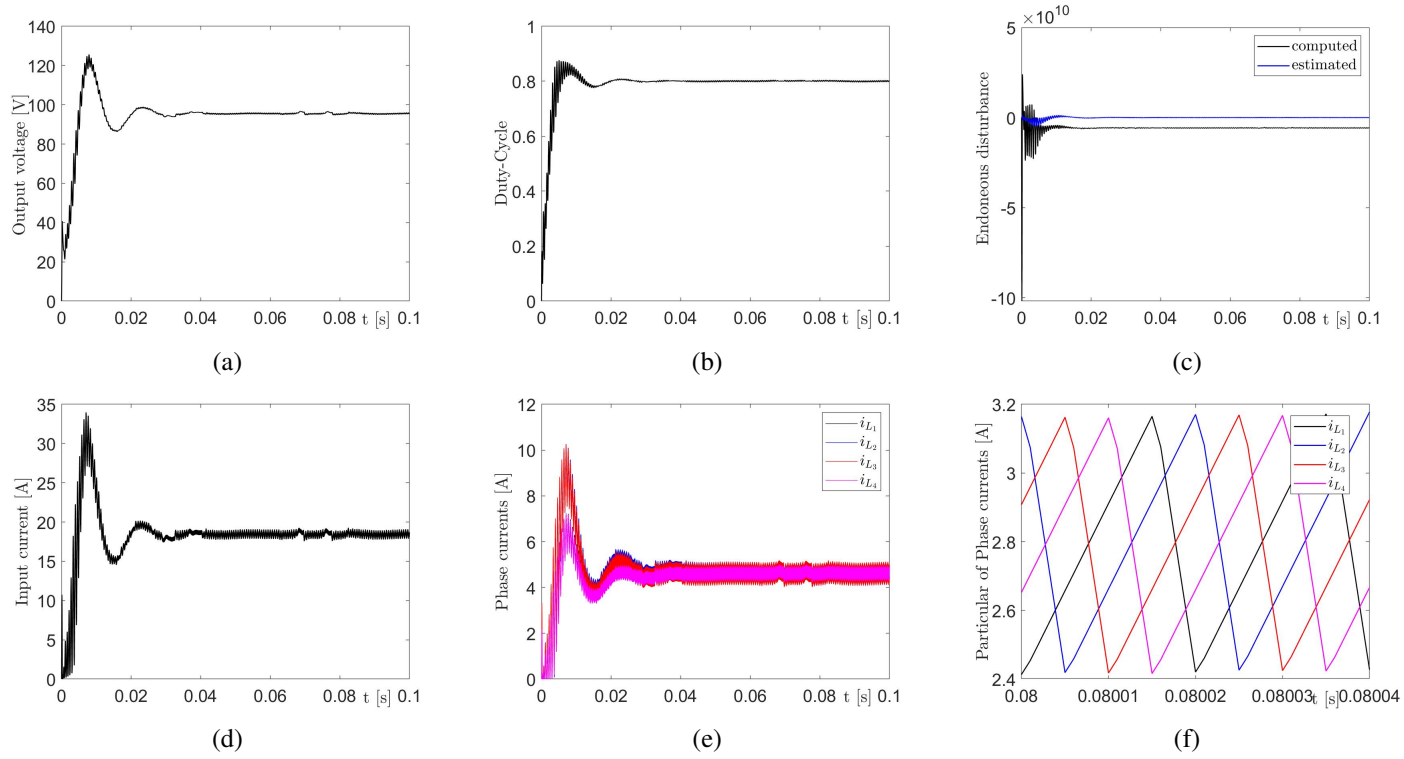

Fig. 3. Test under detuned working conditions: (a) output voltage; (b) duty cycle; (c) computed and estimated disturbance; (d) input current; (e) phase currents; (f) steady-state waveforms of the phase currents.

$1.2L$, and a variation of -30% in R and -10% in C. The results of this second test are given in Fig. 3.

From the results, similar considerations to the ones given above can be given. In particular, it is essential to note that the results in Fig. 3 are pretty similar to Fig. 2, and this confirms that the controller is robust against the above-considered parameter variations.

V. Conclusions

A robust nonlinear control technique has been devised for an interleaved boost converter. It is based on an extended linearization, active compensation of the disturbances, and sliding mode component, giving increased robustness to the closed-loop system. The results show the proposed approach's effectiveness and robustness against the parameter variations, including inductors and capacitors tolerances, and maintaining the advantages of the interleaved topology.

References

[1] B. A. Miwa, D. M. Otten, and M. Schlecht, "High efficiency power factor correction using interleaving techniques," in *Annual Applied Power Electronics Conference and Exposition (APEC 1992)*. IEEE, 1992, pp. 557–568.

[2] A. Sferlazza, C. Albea-Sanchez, and G. Garcia, "A hybrid control strategy for quadratic boost converters with inductor currents estimation," *Control Engineering Practice*, vol. 103, p. 104602, 2020.

[3] C. Albea, A. Sferlazza, F. Gordillo, and F. Gómez-Estern, "Control of power converters with hybrid affine models and pulse-width modulated inputs," *IEEE Transactions on Circuits and Systems I: Regular Papers*, vol. 68, no. 8, pp. 3485–3494, 2021.

[4] F. Alonge, F. D'Ippolito, G. Garraffa, G. C. Giaconia, R. Latona, and A. Sferlazza, "Sliding mode control of quadratic boost converters based on min-type control strategy," *IEEE Access*, 2023.

[5] R. Giral, L. Martinez-Salamero, and S. Singer, "Interleaved converters operation based on CMC," *IEEE Transactions on power electronics*, vol. 14, no. 4, pp. 643–652, 1999.

[6] M. Veerachary, T. Senjyu, and K. Uezato, "Modeling and analysis of interleaved dual boost converter," in *IEEE International Symposium on Industrial Electronics (ISIE 2001)*, vol. 2. IEEE, 2001, pp. 718–722.

[7] O. Hegazy, J. Van Mierlo, and P. Lataire, "Control and analysis of an integrated bidirectional DC/AC and DC/DC converters for plug-in hybrid electric vehicle applications," *Journal of Power Electronics*, vol. 11, no. 4, pp. 408–417, 2011.

[8] C.-M. Lai, C.-T. Pan, and M.-C. Cheng, "High-efficiency modular high step-up interleaved boost converter for DC-microgrid applications," *IEEE Transactions on Industry Applications*, vol. 48, no. 1, pp. 161–171, 2011.

[9] B. Choi, B. Cho, R. Ridley, and F. Lee, "Control strategy for multi-module parallel converter system," in *IEEE Annual Conference on Power Electronics Specialists (PESC 1990)*. IEEE, 1990, pp. 225–234.

[10] Q. Xu, W. Jiang, F. Blaabjerg, C. Zhang, X. Zhang, and T. Fernando, "Backstepping control for large signal stability of high boost ratio interleaved converter interfaced DC microgrids with constant power loads," *IEEE Transactions on Power Electronics*, vol. 35, no. 5, pp. 5397–5407, 2019.

[11] H. Sira-Ramirez and M. Ilic-Spong, "Exact linearization in switched-mode DC-to-DC power converters," *International journal of control*, vol. 50, no. 2, pp. 511–524, 1989.

[12] M. Koundi, Z. El Idrissi, H. El Fadil, F. Z. Belhaj, A. Lassioui, K. Gaouzi, A. Rachid, and F. Giri, "State-feedback control of interleaved buck–boost DC–DC power converter with continuous input current for fuel cell energy sources: Theoretical design and experimental validation," *World Electric Vehicle Journal*, vol. 13, no. 7, p. 124, 2022.

[13] D. Scirè, G. Lullo, and G. Vitale, "Design and modeling of an interleaving boost converter with quasi-saturated inductors for electric vehicles," in *International Conference of Electrical and Electronic Technologies for Automotive (AEIT 2020)*. IEEE, 2020, pp. 1–6.

[14] S. F. Roberto, D. Sciré, G. Lullo, and G. Vitale, "Equivalent circuit modelling of ferrite inductors losses," in *International Forum on Research and Technology for Society and Industry (RTSI 2018)*. IEEE, 2018, pp. 1–4.

[15] J.-J. E. Slotine, W. Li *et al.*, *Applied nonlinear control*. Prentice hall Englewood Cliffs, NJ, 1991, vol. 199, no. 1.

[16] F. Alonge, A. Busacca, M. Calabretta, F. D'Ippolito, A. Fagiolini, G. Garraffa, A. A. Messina, A. Sferlazza, and S. Stivala, "Nonlinear robust control of a quadratic boost converter in a wide operation range, based on extended linearization method," *Electronics*, vol. 11, no. 15, p. 2336, 2022.

[17] T. I. Fossen and J. P. Strand, "Tutorial on nonlinear backstepping: Applications to ship control," 1999.

[18] D. Yoo, S.-T. Yau, and Z. Gao, "Optimal fast tracking observer bandwidth of the linear extended state observer," *International Journal of Control*, vol. 80, no. 1, pp. 102–111, 2007.

[19] B.-Z. Guo and Z.-l. Zhao, "On the convergence of an extended state observer for nonlinear systems with uncertainty," *Systems & Control Letters*, vol. 60, no. 6, pp. 420–430, 2011.